HHS Public Access

Author manuscript

Mol Pharm. Author manuscript; available in PMC 2019 July 02.

Published in final edited form as:

Mol Pharm. 2018 July 02; 15(7): 2721–2731. doi:10.1021/acs.molpharmaceut.8b00237.

Modulating macrophage polarization through CCR2 inhibition and multivalent engagement

Michael B. Deci, **Scott W. Ferguson**, **Sydney L. Scatigno**, and **Juliane Nguyen***

Department of Pharmaceutical Sciences, School of Pharmacy, University at Buffalo, The State University of New York, Buffalo, NY 14214, USA.

Abstract

Excessive or prolonged recruitment of inflammatory monocytes to damaged tissue can significantly worsen patient outcomes. Monocytes migrate to sites of tissue inflammation in response to high local concentrations of CCL2, a chemokine that binds to and signals through the CCR2 receptor. While the role of CCR2 in cellular migration is well studied, it is unclear how CCR2 inhibition affects macrophage polarization and if multivalency can increase downstream signaling effects. Using affinity selection with a phage library, we identified a novel scFv (58C) that binds specifically and with high affinity to the N-terminal domain of CCR2 (K_D = 59.8 nM). The newly identified 58C-scFv bound to native CCR2 expressed on macrophages and MDA-MB-231 cells, inhibited migration, and induced a pro-inflammatory M1-phenotype in macrophages. The M1/M2 macrophage phenotype ratio for monomeric 58C-scFv was significantly increased over the negative control by 1.0×10^4-fold (iNOS/Arg-1), 5.1×10^4-fold (iNOS/Mgl2), 3.4×10^5-fold (IL-6/Arg-1), and 1.7×10^6-fold (IL-6/Mgl2). Multivalent display of 58C-scFv on liposomes further reduced migration of both cell types by 25 to 40% and enhanced M1 polarization by 200% over monomeric 58C-scFv. These studies demonstrate that CCR2 inhibition polarizes macrophages towards an inflammatory M1 phenotype and that multivalent engagement of CCR2 increases the effects of 58C-scFv on polarization and migration. These data provide important insights into the role of multivalency in modulating binding, downstream signaling, and cellular fate.

Keywords

Multivalency; chemokine receptors; multivalency; scFv; cellular migration; phenotype switching

***Corresponding author** Juliane Nguyen, PhD, Assistant Professor, Department of Pharmaceutical Sciences, University at Buffalo, julianen@buffalo.edu, Phone: 716-645-4817.

Author Contribution

MBD and JN conceived and designed the experiments. MBD, SWF, and SS performed the experiments. MBD, SWF, and JN analyzed the data. MDB, SWF, and JN wrote the manuscript. JN supervised the project.

Supporting Information

The Supporting Information is available free of charge on the ACS Publications website at http://pubs.acs.org.

CCR2 expression on cell lines (Suppl. Fig. 1); the effect of 58C-scFv and a commercially available CCR2 antibody on cell migration (Suppl. Fig. 2); the effect of liposomes on cell migration (Suppl. Fig. 3); M1/M2 ratio of macrophages induced with 58C-scFv and compared to two commercially available CCR2 antibodies (Suppl. Fig. 4); the effect of liposomes on M1/M2 ratio (Suppl. Fig. 5); the binding of monomeric and multivalent 58C-scFv to RAW 264.7 cells (Suppl. Fig. 6); the number of 58C-scFv per liposome (Suppl. Table 1), and the hydrodynamic diameter of the different liposome formulations (Suppl. Table 2),

Introduction

Monocytes migrate to sites of inflammation under the influence of chemokines and cytokines. The CCR2 chemokine receptor mediates monocyte egress from the bone marrow under the influence of the chemokine CCL2, which is secreted by cells during inflammatory conditions including myocardial infarction, cancer, atherosclerosis, asthma, and rheumatoid arthritis.[1–3]

At sites of inflammation, monocytes differentiate into functionally polarized macrophages in response to chemokines, cytokines, and other chemical factors. There are two main macrophage phenotypes: M1 and M2.[4] M1 macrophage activation generally occurs in the presence of lipopolysaccharide (LPS),[5] interferon gamma (IFN-γ),[6] and granulocyte-macrophage colony stimulating factor (GM-CSF).[7] M1 macrophages are considered pro-inflammatory and essential early responders at inflammatory disease onset. Macrophage colony-stimulating factor (M-CSF)[7] and specific interleukins (IL-4, IL-13, IL-10)[8–10] induce M2 macrophage activation, which is considered anti-inflammatory. While M2 macrophages are beneficial in the reparative phase of inflammation and contribute to wound healing after myocardial infarction, they can be detrimental in tumors as they promote tumor growth through increased angiogenesis and metastasis and suppression of anti-cancer immune responses.[11–13]

In addition to driving monocyte migration, CCL2 signaling also contributes to M2 macrophage polarization.[14, 15] As the N-terminal domain of the CCR2 receptor captures CCL2 to trigger downstream effects,[16, 17] the CCR2 N-terminal domain represents an ideal target to disrupt the CCR2/CCL2 axis for therapeutic benefit.[18] While several antibodies targeting the CCL2/CCR2 pathway have shown promise in clinical trials in myocardial infarction, atherosclerosis, and cancer,[19–23] none are clinically approved despite initial expectations. Thus, there remains room to capitalize on antibody binding specificity while finding novel ways to improve efficacy. Here we investigated if multivalent display of CCR2-targeting single-chain variable fragment (scFv) antibodies on nanosized liposomes (i) further enhanced binding affinity, and (ii) modulated downstream signaling and cellular phenotypes including migration and macrophage polarization. Phage display was used to screen for N-terminal-binding scFv antibodies. The lead candidate 58C-scFv was subsequently characterized with regard to its binding affinity for CCR2, binding to CCR2-expressing cells, and effect on cellular migration and macrophage polarization. 58C-scFv was also displayed at various ligand densities on liposomes to investigate the effects of multivalency. Our study highlights how nanoparticles functionalized with targeting ligands can not only be used to enhance binding affinity but also to significantly enhance downstream signaling and the therapeutic effects of antibodies. Combining nanocarriers and antibodies has broad implications for significantly enhancing therapeutic capacity that cannot be achieved when each are administered individually.

Materials and Methods

Materials

All chemicals and solvents were purchased from Thermo Fisher Scientific (Waltham, MA), unless otherwise stated.

Phage library screening against CCR2 N-terminal domain

Biotinylated N-terminal CCR2 domain was captured on magnetic streptavidin coated beads and four rounds of affinity selections were performed as previously described.[24] The selection was performed at room temperature using a phage display library that was constructed from peripheral human blood lymphocytes and that expresses single-chain fragments of antibodies. The library was kindly provided by Dr. Mark Sullivan.[25] To identify CCR2 N-terminal domain binders, single bacterial colonies were picked after the fourth round of selection for phage amplification followed by a phage enzyme-linked immunosorbent assay (ELISA). Clones that yielded a signal above background were sequenced and further analyzed with regard to binding affinity.

Protein expression and purification

The 58C-scFv cloned into the pET21a vector (Novagen, Burlington, MA) was expressed in BL-21 (DE3) cells (Lucigen, Middleton, WI). Bacterial cultures were grown overnight at 37°C in 2x YT medium, ampicillin, and 1% glucose. A 1L 2x YT culture was inoculated with 1% of the overnight culture and grown to an OD_{600} of ~0.6. Protein expression was induced with 0.2 mM isopropyl β–D-1-thiogalactopyranoside (IPTG). After an overnight incubation at 24°C, the cells were harvested 18 h post-induction by centrifugation. The cell pellet was resuspended in lysis buffer containing 50 mM Tris, 100 mM KCl, and 2 M urea, pH 8.5. The cell suspension was centrifuged at 9,000 x g for 5 minutes at 4°C and the pellet collected and washed three times with lysis buffer. After the final wash, the pellet was re-suspended in solubilization buffer (50 mM Tris, 100 mM KCl, 5 M guanidine, and 10 mM β-mercaptoethanol, pH 8.5). The solution was incubated at 37°C for 1 h and then centrifuged at 9,000 x g for 10 min at 4°C. The supernatant was collected and diluted 1:10 into refolding buffer containing 50 mM Tris, 500 mM NaCl, 400 mM sucrose, 3 mM reduced glutathione, 0.3 mM oxidized glutathione, 0.5% Triton X-100, 10% glycerol, and 10 mM imidazole, pH 8.5. The solution was stirred at 200 rpm at 4°C for 24 h, after which TALON cobalt beads (Clontech, Mountain View, CA) were equilibrated with refolding buffer and added to the solution. The beads were incubated with the solution and the protein was isolated by immobilized metal affinity chromatography (IMAC).

Enzyme-linked immunosorbent assay (ELISA)

Nunc MaxiSorp 96-well plates were coated with NeutrAvidin at 5 μg/mL and incubated overnight at 4°C. The plate was thoroughly washed with 0.1% PBS-Tween (PBST), and 5 μg/mL biotinylated N-terminal domain CCR2 peptide (MEDNNMLPQFIHGILSTSHSLFTRSIQELDEGATTPYDYDDGEPC; ABclonal, Woburn, MA) added and incubated for 1 h at room temperature. The wells were washed with 0.1% PBST and then blocked with casein blocking buffer for 1 h at room temperature. The wells

were washed with 0.1% PBST followed by incubation of serially diluted scFv for 1 h at room temperature before being washed five times with 0.1% PBST. Washes were followed by the addition of 100 uL of the respective horse-radish peroxidase (HRP)-linked monoclonal antibody (mAb) for 1 h at room temperature with rocking. An anti-M13 mAb was used to detect phages (#27–9421-01, GE healthcare, Chicago, IL) and an anti-flag mAb was used to detect scFv (#A8592, Sigma Aldrich, St. Louis, MO). The wells were washed with 0.1% PBST followed by the addition of TMB-ELISA substrate. After 10 min incubation, 2 M H_2SO_4 was added to stop the reaction. The absorbance was measured at 450 nm with a FilterMax F3 & F5 multi-mode microplate reader (Molecular Devices, Sunnyvale, CA). A 1:1 binding ratio Hill model was used to fit the binding interaction data.

Cell binding analysis by flow cytometry

Cells were detached with 5mM EDTA and re-suspended in PBS to a concentration of 50,000 cells per 300 μL. Cells were plated in a 48-well plate and incubated for 30 min at 4°C. After removing the PBS solution, the cells were incubated with various dilutions of DyLight 650 NHS Ester labeled 58C-scFv for 1 h at 4°C. Cells were washed three times with 5% BSA, detached with EDTA, and analyzed in the APC channel of a MACSQuant Analyzer 10 flow cytometer (Miltenyi Biotec, Bergisch Gladbach, Germany).

Transwell migration assay

Cells were serum starved for 24 h before being detached with 5 mM EDTA in PBS and re-suspended in transwell medium (DMEM without phenol red, 25 mM HEPES, and 0.1% BSA) at a concentration of 70×10^4 cells per 100 μL. Cells were incubated with various concentrations of scFv for 30 min at 4°C and then added to the apical chamber of either a 5 μm (RAW 264.7) or 8 μm (MDA-MB-231) pore transwell plate (Milipore Sigma, Burlington, MA). The basolateral compartment contained 25 nM of CCL2 in serum-free medium to induce chemotaxis. Cells were incubated at 37°C with 5% CO_2 for either 4 h (RAW 264.7) or 21 h (MDA-MB-231). After incubation, the cells in the apical chamber were removed and the wells were placed in a new feeder tray containing pre-warmed cell detachment solution. Wells were incubated with cell detachment buffer for 30 min at 37°C with occasional rocking to detach migrated cells. Then, lysis buffer and dye solution were added to the detachment solution containing the migrated cells. The solution was incubated for 15 min and fluorescence measured on a SpectraMax microplate reader (Molecular Devices) with an excitation/emission of 480/520.

Macrophage polarization

RAW 264.7 mouse macrophages were incubated with either LPS (100 ng/mL), IL-4 (20 ng/mL; PeproTech, Rocky Hill, NJ), or 58C-scFv (1 μM) for 24 h. For the multivalency studies, RAW 264.7 mouse macrophages were first incubated with IL-4 (20 ng/mL) for 24 h to stimulate an M2 phenotype. Following the 24 h incubation, fresh media with 58C-scFv (89 nM) was added to the cells and incubated for an additional 24 h. Total RNA was isolated with QIAzol lysis reagent (Qiagen, Germany) and total cDNA was generated using the New England Biolabs first stand synthesis kit (Ipswich, MA). RNA expression was detected by reverse transcription (RT)-PCR performed with the SYBR Green PCR kit (Qiagen). For each sample, the ΔΔCt value was calculated. Experiments were performed in triplicate. The

primers were: β-actin (forward: 5'-ccctgtatgcctctggtc-3', reverse: 5'-gtctttacggatgtcaacg-3'), iNOS (forward: 5'-tttgcttccatgctaatgcgaaag-3', reverse: 5'-gctctgttgaggtctaaaggctccg-3'), IL-6 (forward: 5'- tgggaaatcgtggaaatgag-3', reverse: 5'-ctgaaggactctggctttgtc-3'), ARG-1 (forward: 5'-cagaagaatggaagagtcag-3', reverse: 5'-cagatatgcagggagtcacc-3'), MGL2 (forward: 5'-agcgggaagagaaaaaccag-3', reverse: 5'-agatgaccaccagtagcaggag-3').

Liposome preparation

All lipids were purchased from Avanti Polar Lipids (Alabaster, AL). Lipids dissolved in chloroform were mixed, dried down to a thin film, and placed under high vacuum for 2 h. Lipid mixtures included DSPC:DGS-NTA(Ni):Chol (50:30:20), DSPC:DGS-NTA(Ni):Chol (70:10:20), and DSPC:DGS-NTA(Ni):Chol (75:5:20). The films were re-hydrated with 1 mL PBS at 60°C and vortexed. The liposomes were sonicated at 60°C for 10 min. The liposomes were extruded through a 100 nm polycarbonate membranes (Avanti Polar Lipids) at 60°C. Liposomes were incubated with a 660:1 molar ratio of DGS-NTA(Ni) lipid to His-tagged 58C-scFv to ensure maximum binding at 4°C overnight. A sepharose CL-6B size exclusion column was used to remove free, unbound 58C-scFv. Fluorescently labeled 58C-scFv was used to determine the amount of scFv bound to liposomes. The low valency formulation had approximately 14 58C-scFvs per liposome, the medium valency formulation had approximately 28 58C-scFvs per liposome, and the high valency formulation had approximately 84 58C-scFvs per liposome (Supplemental Table 1).

Data analysis and statistics

Comparisons between groups were analyzed using one-way ANOVA with post-hoc Dunnett (*$p<0.05$, **$p<0.01$, ***$p<0.001$). All statistical analyses were performed in Prism 7 (GraphPad Software, La Jolla, CA). All experiments were performed in triplicate. The error bars represent standard deviations (SD).

Results

Expression and characterization of 58C-scFv against the N-terminal domain of CCR2

A phage library expressing human scFvs with 2×10^9 diversity was panned against the flexible N-terminal domain of CCR2 (Figure 1A). Binders with an absorbance above background were selected for further characterization. When sequenced, the top five binders all had unique complementarity determining regions (CDRs) (Figure 1B). Phage clone 58C had the highest affinity by phage ELISA and was therefore chosen for subsequent studies (Figure 2A&B). The 58C-scFv protein bound to the CCR2 N-terminus with high affinity (K_D=59.8 nM; Figure 2C) and was recombinantly expressed with a yield of 1 mg/L and a molecular weight of approximately 33 kDa (Figure 2D).

We next assessed if 58C-scFv also bound to cellular CCR2 using RAW 264.7 mouse macrophages and MDA-MB-231 human breast cancer cells,[26] both of which express CCR2 (Supplemental Figure 1A&B). 58C-scFv was fluorescently labeled and bound with concentration dependence to murine macrophages (Figure 2E). Although a CCR2 peptide corresponding to the murine N-terminal domain was used for affinity selection, the human and mouse CCR2 N-terminal domains have 80% sequence similarity. Therefore, we were

interested if the 58C-scFv cross-reacted and bound human CCR2. Indeed, 58C-scFv bound with concentration dependence to human MDA-MB-231 breast cancer cells (Figure 2F). Human embryonic kidney (HEK) cells that are CCR2-negative served as a control.[27] 58C-scFv demonstrated significantly higher binding to CCR2 expressing cells than CCR2-negative HEK cells (Figure 2G).

The effect of 58C-scFv on macrophage and breast cancer cell migration

We next assessed the effect of CCR2-targeting 58C-scFv on macrophage and breast cancer cell migration. Monocytes, macrophages, and breast cancer cells express CCR2 and migrate along the CCR2/CCL2 chemotaxis gradient.[26, 28] RAW 267.4 and MDA-MB-231 cells were incubated with increasing concentrations of 58C-scFv, with CCL2 serving as the chemoattractant. 58C-scFv inhibited migration of breast cancer and macrophage cells by approximately 75% at the highest concentration tested (Figure 3), suggesting that this scFv is specific for the CCL2/CCR2 pathway and acts as a CCR2 antagonist. 58C-scFv demonstrated ~ 40–60% higher inhibition of macrophage migration than a commercially available CCR2-targeted antibody (Supplemental Figure 2).

Because CCR2 receptors cluster at the leading edge of cells when stimulated by CCL2[29] we hypothesized that a multivalent targeting approach would prevent cellular migration better than monomeric 58C-scFv (Figure 4A). We therefore generated liposomes with varying molar ratios of DGS-NTA lipids to control the ligand density of 58C-scFv. The hydrodynamic diameter of the liposomes was between 146 nm and 155 nm as determined by DLS (Supplemental Table 2) and TEM (Figure 4B). 58C-scFv was incubated with liposomes containing 0.05 μM, 0.1 μM, or 0.3 μM of DGS-NTA(Ni) lipid, and the C-terminal hexa-histidine tag of the 58C-scFv was used for binding to the NTA(Ni) lipid. An excess of DGS-NTA (Ni) lipid was used to ensure maximum binding of 58C-scFv. The low valency formulation had approximately 14 58C-scFv per liposome, the medium valency formulation had approximately 28 58C-scFv per liposome, and the high valency formulation had approximately 84 58-scFv per liposome. Total protein was kept constant across conditions to assess how ligand density affected cellular migration. For the valency study, we normalized to the monomeric 58C-scFv, which already demonstrated a 1.75-fold and 1.87-fold enhancement over negative control for MDA-MB-231 and RAW 264.7 cells at a dose of 88.9 nM, respectively. Liposomes without 58C-scFv were not significantly different from the negative control (Supplemental Figure 3A&B). Multivalent display of 58C-scFv at low, medium, and high valency further inhibited migration in RAW 264.7 and MDA-MB-231 cells (Figure 4C&D). At the highest valency, there was a significant 25% reduction in RAW 264.7 migration compared to free 58C-scFv. For MDA-MB-231 cells, multivalent display of 58C-scFv resulted in a significant 40% reduction in migration compared to free monomeric 58C-scFv.

The effect of 58C-scFv on macrophage polarization

Cancer cell secretion of CCL2, a CCR2 agonist, into the tumor microenvironment can polarize macrophages to an M2 phenotype.[14, 15] The CCR2-targeting 58C-scFv was incubated with RAW 264.7 macrophages to test our hypothesis that CCR2 antagonism would polarize macrophages toward an M1 phenotype. Macrophages were polarized to M1

(iNOS and IL-6 expressing)[30–33] by the addition of LPS, or to M2 (Arg-1 and Mgl-2 expressing)[33–36] by the addition of IL-4. As expected, LPS induced M1 gene expression and downregulated Mgl2 gene expression compared to the untreated control (Figure 5A). The 58C-scFv induced a quantitatively similar expression pattern to that of LPS, suggesting that 58C-scFv polarized macrophages to the M1 phenotype (Figure 5B). IL-4 increased both Arg-1 and Mgl2 gene expression compared to the untreated control (Figure 5C). Even in the presence of IL-4, the 58C-scFv still downregulated the M2 gene expression and upregulated M1 gene expression compared to the IL-4 only control (Figure 5D). For cancer therapy, it is beneficial to have macrophages with M1 rather than M2 phenotypes because M2 macrophages have a tumor-promoting phenotype. To this end, we used four genes (two M1 and two M2 genes) to assay for the relative phenotype of macrophages upon different conditions (Figure 5E). The ratios of M1 and M2 genes corroborated the phenotype of macrophages suggested from our single gene analysis (Figure 5F). For LPS, three of the four M1/M2 ratios were significantly above control, suggesting the macrophages had an M1 phenotype. For IL-4, all four M1/M2 ratios were significantly below control, suggesting the macrophages had an M2 phenotype. The 58C-scFv had similar fold-changes as the LPS group with three of the four ratios being statistically significant. The M1/M2 ratio for monomeric 58C-scFv was significantly increased over the negative control by 1.0×10^4-fold (iNOS/Arg-1), 5.1×10^4-fold (iNOS/Mgl2), 3.4×10^5-fold (IL-6/Arg-1), and 1.7×10^6-fold (IL-6/Mgl2) (Figure 5F). When 58C-scFv was co-incubated with the M2 promoting agent, IL-4, two of the ratios were significantly increased over control, with a clear trend for the third ratio (iNOS/Mgl2) having an M1 phenotype. Co-incubation of the IL-4 and 58C-scFv demonstrated 58C-scFv is able to polarize macrophages back to an M1 phenotype. 58C-scFv significantly increased the M1/M2 ratios in macrophages by 3- to 9-fold compared to two commercially available CCR2-targeted antibodies (Supplemental Figure 4).

Impact of 58C-scFv multivalency on macrophage polarization

We next investigated the effect of multivalency on macrophage polarization. Macrophages were first polarized to an M2 phenotype with IL-4 followed by incubation with different ligand densities of 58C-scFv (Figure 6A). Monomeric 58C-scFv and all liposome-bound 58C-scFv shifted the macrophage phenotype from M2 to M1, as measured by the M1/M2 gene ratio (Figure 6B-E). Four different ratios (iNOS/Arg-1, iNOS/Mgl2, IL-6/Arg-1, and IL-6/Mgl2) were compared across conditions. The M1/M2 ratios for the liposomes without 58C-scFv were not statistically different from the negative control (Supplemental Figure 5A-D).

Moreover, the three different ligand densities of 58C-scFv outperformed the monomeric 58C-scFv with a trend for increasing M1/M2 ratio from the lowest to the highest valency. Compared to monomeric 58C-scFv, the highest valency produced 2.2-fold, 2.1-fold, 1.6-fold, and 1.3-fold higher M1/M2 ratios for IL-6/Mgl2, IL-6/Arg-1, iNOS/Mgl2, and iNOS/Arg-1, respectively. Further, the IL-6/Mgl2, IL-6/Arg-1, and iNOS/Mgl2 ratios were significantly higher than the monomeric 58C-scFv at the highest valency (Figure 6). The medium valency was also significantly higher for the IL-6/ARG-1 ratio. The monomeric 58C-scFv strongly polarized macrophages to an M1 phenotype, but to a lesser degree than multivalent 58C-scFv.

Discussion

Inflammatory monocytes contribute to the progression of many pathophysiological conditions including wound healing, myocardial infarction, rheumatoid arthritis, and cancer. Monocyte and macrophage mobilization to the inflamed site is in part mediated by the CCL2/CCR2 chemotaxis gradient. Inhibiting the excessive migration of inflammatory monocytes to the disease site has been shown to improve wound healing, reduce infarct size after myocardial infarction, and inhibit tumor growth and progression in many types of cancer. However, despite promising (pre-)clinical data, there are no approved antibody-based therapeutics against CCR2. The lack of clinical success can partially be attributed to insufficient inhibition of CCR2-mediated migration.[37] Furthermore, there have been no targeted or multivalent nanocarriers approved by the FDA because of poor understanding for nanocarrier-target interactions.[38, 39]

We hypothesized that multivalent display of antibodies would not only result in increased binding affinity (~8-fold by cell-binding assay; Supplemental Figure 6), but could also have a positive effect on downstream signaling events and other receptor-mediated effects. Multivalent display has been demonstrated by a host of carriers including lipid nanoparticles,[40] polymers,[41] and proteins.[42] Although it is widely accepted that multivalent ligand display has many benefits for nanomedicine such as increased binding affinity, enhanced endocytosis, and ‘superselective’ targeting,[38, 43–48] the effects of ligand multivalency on the functional activity of receptors and downstream signaling events are underappreciated and underexplored.

To test our hypothesis, we first used phage display screening to identify novel scFvs targeting the N-terminal domain of CCR2. Of the top binders, the 58C-scFv bound with high affinity to the N-terminal domain peptide (K_D=59.8 nM). Further, 58C-scFv also bound to CCR2-positive murine macrophages and CCR2-positive human breast cancer cells. This cross-species reactivity is useful for future experimental and clinical applications. In a migration assay, monomeric 58C-scFv significantly inhibited migration of RAW264.7 macrophages and metastatic breast cancer cells, indicating that 58C-scFv acts as a CCR2-antagonist.

Mechanistically, CCL2-mediated cellular migration involves CCR2 clustering, so we hypothesized that multivalent display of 58C-scFv would more favorably prevent migration. Our data showed that multivalent display of 58C-scFv on liposomes had a stronger inhibitory effect on macrophage migration than monomeric scFv at all ligand densities tested. The multivalent 58C-scFv outperformed the monomeric form and reduced macrophage and breast cell migration by ~40% compared to controls. The data suggest that multivalent display of a CCR2-antagonist is beneficial for inhibiting cellular migration compared to a monomeric CCR2 antagonist. Additionally, increasing the ligand density improved CCR2 antagonism. These findings have translational potential for *in vivo* targeting in diseases where the migration of immune cells to inflamed tissues is detrimental to patient outcomes. In future studies, we plan to investigate the benefit of multivalent display of a CCR2-antagonist *in vivo*.

Since CCL2 not only acts as a chemoattractant, but also promotes M2 polarization in the tumor microenvironment, we examined if 58C-scFv binding to the CCR2 N-terminal domain affects macrophage polarization.[14, 15] Excitingly, 58C-scFv not only inhibited monocyte migration but also induced M1 macrophage polarization. Further, 58C-scFv was also able to polarize macrophages to an M1 phenotype even in the presence of IL-4. These observations are in line with CCR2 antagonism.

We also assessed the effect of multivalency and ligand density in respect to macrophage polarization using the same liposome strategy. Like many receptors, clustering is a vital step in CCR2 activation and signaling and can be induced through multivalent display of antibodies.[29, 38, 49] We first polarized macrophages with IL-4 to an M2 phenotype. Aside from polarizing M1 to M2 macrophages via STAT6 activation, IL-4 also increases the expression of CCL2 in macrophages,[50] which in turn regulates the extent of macrophage polarization. Inhibiting binding of CCL2 to CCR2 has been shown to increase the expression of M1-associated genes.[51] Multivalent display of 58C-scFv was able to recover macrophages from an M2 phenotype and polarize them to an M1 phenotype. While monomeric 58C-scFv was able to induce a phenotype switch in macrophages from M2 to M1, multivalent 58C-scFv was superior to the free 58C-scFv at all ligand densities. Liposomes with the highest density of 58C-scFv more strongly induced M1 polarization than liposomes with medium and lower 58C-scFv ligand density. Liposomes without 58C-scFv demonstrated no effect on macrophage polarization.

The ability of the multivalent 58C-scFv to elicit greater M1 macrophage polarization and reduce cell migration compared to traditional monomeric protein is relevant for the clinical application of therapeutic proteins (Figure 7). With a multivalent display strategy, proteins traditionally administered in monomeric form could be administered at lower doses and with increased efficacy. This also equates to decreased production time and costs. Multivalency can also enhance selectivity, especially at low receptor expression,[52] which limits off-target toxicity. Attachment of 58C-scFv to NTA-lipids was used as a proof-of-concept method to study the impact of multivalency on downstream signaling. However, for *in vivo* conditions the binding affinity between the His-tag and the NTA-lipid is likely not sufficiently strong.[53] Thus, conjugation methods based on maleimide-chemistry would be a more suitable attachment technique for *in vivo* stability.[54]

The observed effects of 58C-scFv to inhibit migration as well as polarize macrophages to an M1 phenotype are highly relevant for tumor therapy. Macrophage plasticity allows for drastic changes in phenotypes by sensing their environment and external cues.[30, 50, 55] Stimuli in the tumor microenvironment differentiate macrophages to an M2-like phenotype, also known as tumor-associated macrophages (TAMs). TAMs promote tumor growth by suppressing the immune system, forming new blood vessels, increasing cancer cell growth, and enhancing migration and metastasis.[11–13, 56, 57] Given their multi-faceted and malignant effects, there have been many recent efforts to abolish TAMs from the tumor microenvironment.[58] However, without complete blockade of macrophage infiltration, there efforts remain frustratingly ineffective. Thus, a strategy that both inhibit migration as well as polarizing TAMs to the tumor-suppressor phenotype (M1) is highly desirable. Future studies

investigating multivalent display of CCR2-antogonists in the tumor microenvironment are warranted.

Aside from affecting tumor growth, the progression of numerous diseases, including but not limited to ischemic heart diseases, atherosclerosis, and asthma, is highly dependent on the timely switch from the M1 to M2 phenotype or vice versa.[59] This study introduces a novel CCR2-targeting 58C-scFv that effectively inhibits the migration of CCR2-positive cells and polarizes macrophages to an M1 phenotype. To our knowledge this is the first study to report that inhibiting CCR2 also induces macrophage polarization towards a M1 phenotype. Additionally, we highlight the substantial benefits of a multivalent approach when intervening in signaling pathways. Specifically, the data demonstrate how multivalent display of antibodies using nanoparticles is a highly effective way to enhance the inhibitory effects on receptor-mediated cell migration. Ultimately, the approach taken here could be applied to a wide range of receptors, targeting ligands, and nanocarriers. Our multivalent strategy provides a novel means to significantly enhance the therapeutic potential of antibodies while at the same time capitalizing on the unique carrier and drug loading properties of nanoparticles.

Supplementary Material

Refer to Web version on PubMed Central for supplementary material.

Acknowledgements

We acknowledge funding from the NIH through awards: R21HL126082, R21EB021454 and R01EB023262. We thank Dr. Mark Sullivan for providing us with the phage display library. We thank Dr. Brian Kay (University of Illinois at Chicago) and Dr. Renhua Huang for training in techniques related to phage display and screening. We thank Brian McIntyre (University of Rochester) for the TEM measurements of liposomes. Michael Deci and Scott Ferguson acknowledge funding by the Allan Barnett Fellowship.

References

1. Pittet MJ; Swirski FK Monocytes link atherosclerosis and cancer. Eur J Immunol 2011, 41, (9), 2519–22. [PubMed: 21952809]
2. Talbot J; Bianchini FJ; Nascimento DC; Oliveira RD; Souto FO; Pinto LG; Peres RS; Silva JR; Almeida SC; Louzada-Junior P; Cunha TM; Cunha FQ; Alves-Filho JC CCR2 Expression in Neutrophils Plays a Critical Role in Their Migration Into the Joints in Rheumatoid Arthritis. Arthritis Rheumatol 2015, 67, (7), 1751–9. [PubMed: 25779331]
3. Heck S; Nguyen J; Le DD; Bals R; Dinh QT Pharmacological Therapy of Bronchial Asthma: The Role of Biologicals. Int Arch Allergy Immunol 2015, 168, (4), 241–52. [PubMed: 26895179]
4. Italiani P; Boraschi D From Monocytes to M1/M2 Macrophages: Phenotypical vs. Functional Differentiation. Front Immunol 2014, 5, (1), 514. [PubMed: 25368618]
5. Classen A; Lloberas J; Celada A, Macrophage activation: classical versus alternative. 2009; Vol. 531, p 29–43.
6. Lyamina SV; Kruglov SV; Vedenikin TY; Borodovitsyna OA; Suvorova IA; Shimshelashvili SL; Malyshev IY Alternative Reprogramming of M1/M2 Phenotype of Mouse Peritoneal Macrophages In Vitro with Interferon-gamma and Interleukin-4. Bulletin of Experimental Biology and Medicine 2012, 152, (4), 548–551. [PubMed: 22803130]
7. Yamane K; Leung KP Rabbit M1 and M2 macrophages can be induced by human recombinant GM-CSF and M-CSF. Febs Open Bio 2016, 6, (9), 945–953.

8. Egawa M; Mukai K; Yoshikawa S; Iki M; Mukaida N; Kawano Y; Minegishi Y; Karasuyama H Inflammatory monocytes recruited to allergic skin acquire an anti-inflammatory M2 phenotype via basophil-derived interleukin-4. Immunity 2013, 38, (3), 570–80. [PubMed: 23434060]

9. Martinez FO; Gordon S The M1 and M2 paradigm of macrophage activation: time for reassessment. F1000Prime Rep 2014, 6, (13), 13. [PubMed: 24669294]

10. Mantovani A; Sozzani S; Locati M; Allavena P; Sica A Macrophage polarization: tumor-associated macrophages as a paradigm for polarized M2 mononuclear phagocytes. Trends in Immunology 2002, 23, (11), 549–555. [PubMed: 12401408]

11. Messmer MN; Netherby CS; Banik D; Abrams SI Tumor-induced myeloid dysfunction and its implications for cancer immunotherapy. Cancer Immunol Immunother 2015, 64, (1), 1–13. [PubMed: 25432147]

12. Yoshikawa K; Mitsunaga S; Kinoshita T; Konishi M; Takahashi S; Gotohda N; Kato Y; Aizawa M; Ochiai A Impact of tumor-associated macrophages on invasive ductal carcinoma of the pancreas head. Cancer Sci 2012, 103, (11), 2012–20. [PubMed: 22931216]

13. Condeelis J; Pollard JW Macrophages: obligate partners for tumor cell migration, invasion, and metastasis. Cell 2006, 124, (2), 263–6. [PubMed: 16439202]

14. Li N; Qin J; Lan L; Zhang H; Liu F; Wu Z; Ni H; Wang Y PTEN inhibits macrophage polarization from M1 to M2 through CCL2 and VEGF-A reduction and NHERF-1 synergism. Cancer Biol Ther 2015, 16, (2), 297–306. [PubMed: 25756512]

15. Roca H; Varsos ZS; Sud S; Craig MJ; Ying C; Pienta KJ CCL2 and interleukin-6 promote survival of human CD11b+ peripheral blood mononuclear cells and induce M2-type macrophage polarization. J. Biol. Chem. 2009, 284, (49), 34342–54. [PubMed: 19833726]

16. Monteclaro FS; Charo IF The amino-terminal domain of CCR2 is both necessary and sufficient for high affinity binding of monocyte chemoattractant protein 1 - Receptor activation by a pseudo-tethered ligand. J. Biol. Chem 1997, 272, (37), 23186–23190. [PubMed: 9287323]

17. Prossnitz ER; Gilbert TL; Chiang S; Campbell JJ; Qin S; Newman W; Sklar LA; Ye RD Multiple activation steps of the N-formyl peptide receptor. Biochemistry 1999, 38, (8), 2240–7. [PubMed: 10029516]

18. Han KH; Green SR; Tangirala RK; Tanaka S; Quehenberger O Role of the first extracellular loop in the functional activation of CCR2. The first extracellular loop contains distinct domains necessary for both agonist binding and transmembrane signaling. J. Biol. Chem 1999, 274, (45), 32055–62. [PubMed: 10542238]

19. Nywening TM; Wang-Gillam A; Sanford DE; Belt BA; Panni RZ; Cusworth BM; Toriola AT; Nieman RK; Worley LA; Yano M; Fowler KJ; Lockhart AC; Suresh R; Tan BR; Lim KH; Fields RC; Strasberg SM; Hawkins WG; DeNardo DG; Goedegebuure SP; Linehan DC Targeting tumour-associated macrophages with CCR2 inhibition in combination with FOLFIRINOX in patients with borderline resectable and locally advanced pancreatic cancer: a single-centre, open-label, dose-finding, non-randomised, phase 1b trial. Lancet Oncol 2016, 17, (5), 651–62. [PubMed: 27055731]

20. Sanford DE; Belt BA; Panni RZ; Mayer A; Deshpande AD; Carpenter D; Mitchem JB; Plambeck-Suess SM; Worley LA; Goetz BD; Wang-Gillam A; Eberlein TJ; Denardo DG; Goedegebuure SP; Linehan DC Inflammatory monocyte mobilization decreases patient survival in pancreatic cancer: a role for targeting the CCL2/CCR2 axis. Clin Cancer Res 2013, 19, (13), 3404–15. [PubMed: 23653148]

21. Gilbert J; Lekstrom-Himes J; Donaldson D; Lee Y; Hu M; Xu J; Wyant T; Davidson M; Group MLNS Effect of CC chemokine receptor 2 CCR2 blockade on serum C-reactive protein in individuals at atherosclerotic risk and with a single nucleotide polymorphism of the monocyte chemoattractant protein-1 promoter region. Am J Cardiol 2011, 107, (6), 906–11. [PubMed: 21247529]

22. Lim SY; Yuzhalin AE; Gordon-Weeks AN; Muschel RJ Targeting the CCL2-CCR2 signaling axis in cancer metastasis. Oncotarget 2016, 7, (19), 28697–710. [PubMed: 26885690]

23. Wang-Gillam A; Nywening TM; Sanford DE; Lockhart AC; Suresh R; Tan BR; Lim KH; Sorscher S; Fowler K; Amin MA; Roshal A; Adkins D; Nieman R; Panni RZ; DeNardo DG; Goedegebuure PS; Hawkins WG; Fields RC; Strasberg SM; Linehan D Phase IB study of FOLFIRINOX plus

PF-04136309 in patients with borderline resectable and locally advanced pancreatic adenocarcinoma (PC). Journal of Clinical Oncology 2015, 33, (3).

24. Huang R; Gorman KT; Vinci CR; Dobrovetsky E; Graslund S; Kay BK Streamlining the Pipeline for Generation of Recombinant Affinity Reagents by Integrating the Affinity Maturation Step. Int J Mol Sci 2015, 16, (10), 23587–603. [PubMed: 26437402]
25. Haidaris CG; Malone J; Sherrill LA; Bliss JM; Gaspari AA; Insel RA; Sullivan MA Recombinant human antibody single chain variable fragments reactive with Candida albicans surface antigens. J Immunol Methods 2001, 257, (1–2), 185–202. [PubMed: 11687252]
26. Fang WB; Jokar I; Zou A; Lambert D; Dendukuri P; Cheng N CCL2/CCR2 Chemokine Signaling Coordinates Survival and Motility of Breast Cancer Cells through Smad3 Protein- and p42/44 Mitogen-activated Protein Kinase (MAPK)-dependent Mechanisms. J. Biol. Chem 2012, 287, (43), 36593–36608. [PubMed: 22927430]
27. Atwood BK; Lopez J; Wager-Miller J; Mackie K; Straiker A Expression of G protein-coupled receptors and related proteins in HEK293, AtT20, BV2, and N18 cell lines as revealed by microarray analysis. BMC Genomics 2011, 12, (14), 14. [PubMed: 21214938]
28. Qian BZ; Li J; Zhang H; Kitamura T; Zhang J; Campion LR; Kaiser EA; Snyder LA; Pollard JW CCL2 recruits inflammatory monocytes to facilitate breast-tumour metastasis. Nature 2011, 475, (7355), 222–5. [PubMed: 21654748]
29. Nieto M; Frade JM; Sancho D; Mellado M; Martinez AC; Sanchez-Madrid F Polarization of chemokine receptors to the leading edge during lymphocyte chemotaxis. J Exp Med 1997, 186, (1), 153–8. [PubMed: 9207004]
30. Davis MJ; Tsang TM; Qiu YF; Dayrit JK; Freij JB; Huffnagle GB; Olszewski MA Macrophage M1/M2 Polarization Dynamically Adapts to Changes in Cytokine Microenvironments in Cryptococcus neoformans Infection. Mbio 2013, 4, (3).
31. Lisi L; Ciotti GMP; Braun D; Kalinin S; Curro D; Dello Russo C; Coli A; Mangiola A; Anile C; Feinstein DL; Navarra P Expression of iNOS, CD163 and ARG-1 taken as M1 and M2 markers of microglial polarization in human glioblastoma and the surrounding normal parenchyma. Neuroscience Letters 2017, 645, (1), 106–112. [PubMed: 28259657]
32. Edin S; Wikberg ML; Dahlin AM; Rutegard J; Oberg A; Oldenborg PA; Palmqvist R The distribution of macrophages with a M1 or M2 phenotype in relation to prognosis and the molecular characteristics of colorectal cancer. PLoS One 2012, 7, (10), e47045. [PubMed: 23077543]
33. Jablonski KA; Amici SA; Webb LM; Ruiz-Rosado Jde D; Popovich PG; Partida-Sanchez S; Guerau-de-Arellano M Novel Markers to Delineate Murine M1 and M2 Macrophages. PLoS One 2015, 10, (12), e0145342. [PubMed: 26699615]
34. Raes G; Brys L; Dahal BK; Brandt J; Grooten J; Brombacher F; Vanham G; Noel W; Bogaert P; Boonefaes T; Kindt A; Van den Bergh R; Leenen PJM; De Baetselier P; Ghassabeh GH Macrophage galactose-type C-type lectins as novel markers for alternatively activated macrophages elicited by parasitic infections and allergic airway inflammation. Journal of Leukocyte Biology 2005, 77, (3), 321–327. [PubMed: 15591125]
35. Hu W; Jiang Z; Zhang Y; Liu Q; Fan J; Luo N; Dong X; Yu X Characterization of infiltrating macrophages in high glucose-induced peritoneal fibrosis in rats. Mol Med Rep 2012, 6, (1), 93–9. [PubMed: 22552745]
36. Yu E; Goto M; Ueta H; Kitazawa Y; Sawanobori Y; Kariya T; Sasaki M; Matsuno K Expression of area-specific M2-macrophage phenotype by recruited rat monocytes in duct-ligation pancreatitis. Histochem Cell Biol 2016, 145, (6), 659–73. [PubMed: 26860866]
37. Lebre MC; Vergunst CE; Choi IYK; Aarrass S; Oliveira ASF; Wyant T; Horuk R; Reedquist KA; Tak PP Why CCR2 and CCR5 Blockade Failed and Why CCR1 Blockade Might Still Be Effective in the Treatment of Rheumatoid Arthritis. Plos One 2011, 6, (7).
38. Deci MB; Liu M; Dinh QT; Nguyen J Precision engineering of targeted nanocarriers. Wiley Interdiscip Rev Nanomed Nanobiotechnol 2018, e1511, (1).
39. Tinkle S; McNeil SE; Muhlebach S; Bawa R; Borchard G; Barenholz YC; Tamarkin L; Desai N Nanomedicines: addressing the scientific and regulatory gap. Ann N Y Acad Sci 2014, 1313, (35), 35–56. [PubMed: 24673240]

40. Nguyen J; Sievers R; Motion JPM; Kivimae S; Fang QZ; Lee RJ Delivery of Lipid Micelles into Infarcted Myocardium Using a Lipid-Linked Matrix Metalloproteinase Targeting Peptide. Molecular Pharmaceutics 2015, 12, (4), 1150–1157. [PubMed: 25642730]
41. Lamm RJ; Lim EB; Weigandt KM; Pozzo LD; White NJ; Pun SH Peptide valency plays an important role in the activity of a synthetic fibrin-crosslinking polymer. Biomaterials 2017, 132, (96), 96–104. [PubMed: 28411452]
42. Deci MB; Ferguson SW; Liu M; Peterson DC; Koduvayur SP; Nguyen J Utilizing clathrin triskelions as carriers for spatially controlled multi-protein display. Biomaterials 2016, 108, (120), 120–128. [PubMed: 27627809]
43. Dubacheva GV; Curk T; Auzely-Velty R; Frenkel D; Richter RP Designing multivalent probes for tunable superselective targeting. Proceedings of the National Academy of Sciences of the United States of America 2015, 112, (18), 5579–5584. [PubMed: 25901321]
44. Mammen M; Choi SK; Whitesides GM Polyvalent interactions in biological systems: Implications for design and use of multivalent ligands and inhibitors. Angewandte Chemie-International Edition 1998, 37, (20), 2755–2794.
45. Riley RS; Day ES Frizzled7 Antibody-Functionalized Nanoshells Enable Multivalent Binding for Wnt Signaling Inhibition in Triple Negative Breast Cancer Cells. Small 2017, 13, (26).
46. Fakhari A; Baoum A; Siahaan TJ; Le KB; Berkland C Controlling ligand surface density optimizes nanoparticle binding to ICAM-1. J. Pharm. Sci 2011, 100, (3), 1045–56. [PubMed: 20922813]
47. Merkel OM; Germershaus O; Wada CK; Tarcha PJ; Merdan T; Kissel T Integrin alpha(nu)beta(3) Targeted Gene Delivery Using RGD Peptidomimetic Conjugates with Copolymers of PEGylated Poly(ethylene imine). Bioconjugate Chem. 2009, 20, (6), 1270–1280.
48. Vogel J; Bendas G; Bakowsky U; Hummel G; Schmidt RR; Kettmann U; Rothe U The role of glycolipids in mediating cell adhesion: a flow chamber study. Biochim. Biophys. Acta 1998, 1372, (2), 205–15. [PubMed: 9675282]
49. Terashima Y; Onai N; Murai M; Enomoto M; Poonpiriya V; Hamada T; Motomura K; Suwa M; Ezaki T; Haga T; Kanegasaki S; Matsushima K Pivotal function for cytoplasmic protein FROUNT in CCR2-mediated monocyte chemotaxis. Nat Immunol 2005, 6, (8), 827–35. [PubMed: 15995708]
50. Wang N; Liang H; Zen K Molecular mechanisms that influence the macrophage m1-m2 polarization balance. Front Immunol 2014, 5, (614), 614. [PubMed: 25506346]
51. Sierra-Filardi E; Nieto C; Dominguez-Soto A; Barroso R; Sanchez-Mateos P; Puig-Kroger A; Lopez-Bravo M; Joven J; Ardavin C; Rodriguez-Fernandez JL; Sanchez-Torres C; Mellado M; Corbi AL CCL2 shapes macrophage polarization by GM-CSF and M-CSF: identification of CCL2/CCR2-dependent gene expression profile. J Immunol 2014, 192, (8), 3858–67. [PubMed: 24639350]
52. Martinez-Veracoechea FJ; Frenkel D Designing super selectivity in multivalent nano-particle binding. Proceedings of the National Academy of Sciences of the United States of America 2011, 108, (27), 10963–10968. [PubMed: 21690358]
53. Platt V; Huang Z; Cao L; Tiffany M; Riviere K; Szoka FC Jr. Influence of multivalent nitrilotriacetic acid lipid-ligand affinity on the circulation half-life in mice of a liposome-attached His6-protein. Bioconjug Chem 2010, 21, (5), 892–902. [PubMed: 20384362]
54. Xu L; Huang CC; Huang W; Tang WH; Rait A; Yin YZ; Cruz I; Xiang LM; Pirollo KF; Chang EH Systemic tumor-targeted gene delivery by anti-transferrin receptor scFv-immunoliposomes. Mol Cancer Ther 2002, 1, (5), 337–46. [PubMed: 12489850]
55. Stout RD; Jiang CC; Matta B; Tietzel I; Watkins SK; Suttles J Macrophages sequentially change their functional phenotype in response to changes in microenvironmental influences. Journal of Immunology 2005, 175, (1), 342–349.
56. Hu W; Li X; Zhang C; Yang Y; Jiang J; Wu C Tumor-associated macrophages in cancers. Clin Transl Oncol 2016, 18, (3), 251–8. [PubMed: 26264497]
57. Liu CY; Xu JY; Shi XY; Huang W; Ruan TY; Xie P; Ding JL M2-polarized tumor-associated macrophages promoted epithelial-mesenchymal transition in pancreatic cancer cells, partially through TLR4/IL-10 signaling pathway. Lab. Invest 2013, 93, (7), 844–54. [PubMed: 23752129]

58. Cieslewicz M; Tang J; Yu JL; Cao H; Zavaljevski M; Motoyama K; Lieber A; Raines EW; Pun SH Targeted delivery of proapoptotic peptides to tumor-associated macrophages improves survival. Proc Natl Acad Sci U S A 2013, 110, (40), 15919–24. [PubMed: 24046373]

59. Hunter P The inflammation theory of disease. The growing realization that chronic inflammation is crucial in many diseases opens new avenues for treatment. EMBO Rep 2012, 13, (11), 968–70. [PubMed: 23044824]

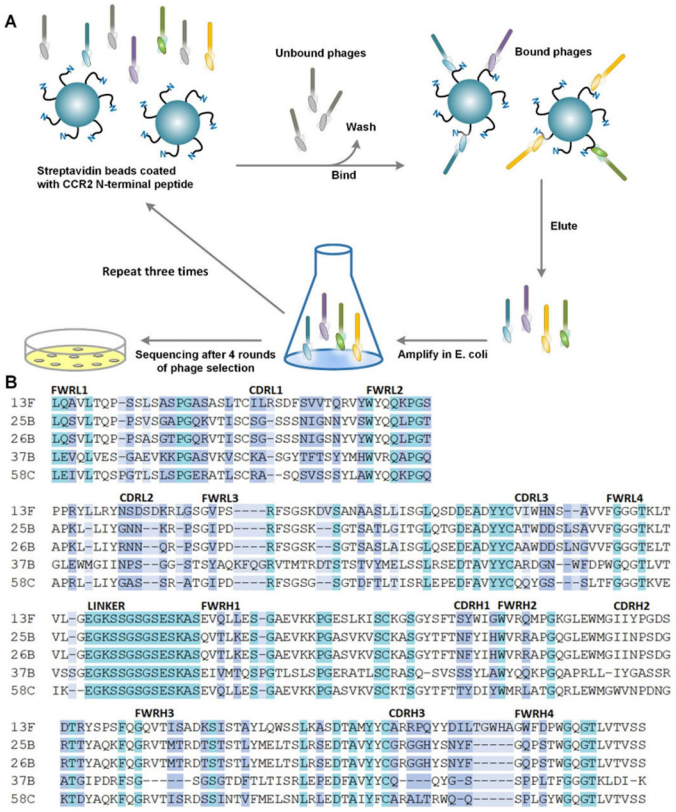

Figure 1.

(A) Schematic of phage display screening against the CCR2 N-terminal peptide domain. **(B)** The top five clones showing the highest affinity to the CCR2 N-terminus were sequenced. The framework regions (light and heavy chains; FWRL and FWRH) and complementarity determining regions (light and heavy chains; CDRL and CDRH) are aligned and compared. Color indicates exact match (teal), partial matches (white), similar amino-acid properties (purple), or dissimilar amino acids (light blue).

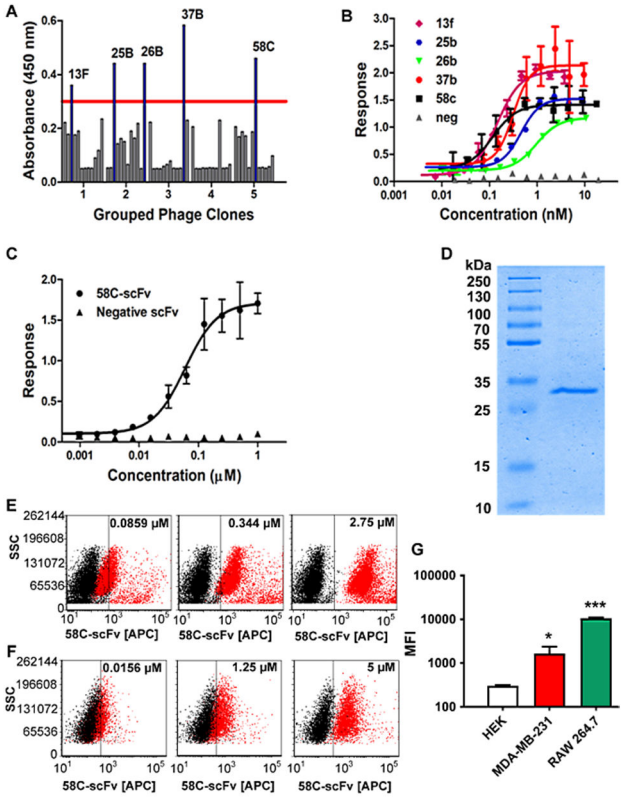

Figure 2. Identification and characterization of 58C-scFv binding to CCR2.

(**A**) Phage ELISA of clones generated through affinity selection using a scFv library. (**B**) Binding affinity of the top 5 phage clones as analyzed by ELISA (**C**) Binding of the recombinantly expressed 58C-scFv to the N-terminal domain of CCR2 as analyzed by ELISA (K_D = 59.8 ± 13.9 nM) (**D**) SDS-PAGE of purified 58C-scFv (MW approx. 33 kDa) on a 12% gel: ladder (lane 1), 58C-scFv sample (lane 2). (**E**) 58C-scFv binding to RAW 264.7 (**F**) and MDA-MB-231 cells was concentration-dependent. (**G**) Mean fluorescent intensity (MFI) following incubation of HEK, MDA-MB-231, and Raw264.7 cells with the DyLight-650 labeled 58C-scFv. The MFI was determined at 2.5 μM for MDA-MB-231 and HEK, and RAW 264.7 cells. Data are represented as mean ± sd, *p<0.05, **p<0.01, ***p<0.001 with one-way ANOVA followed by Dunnett's post-test.

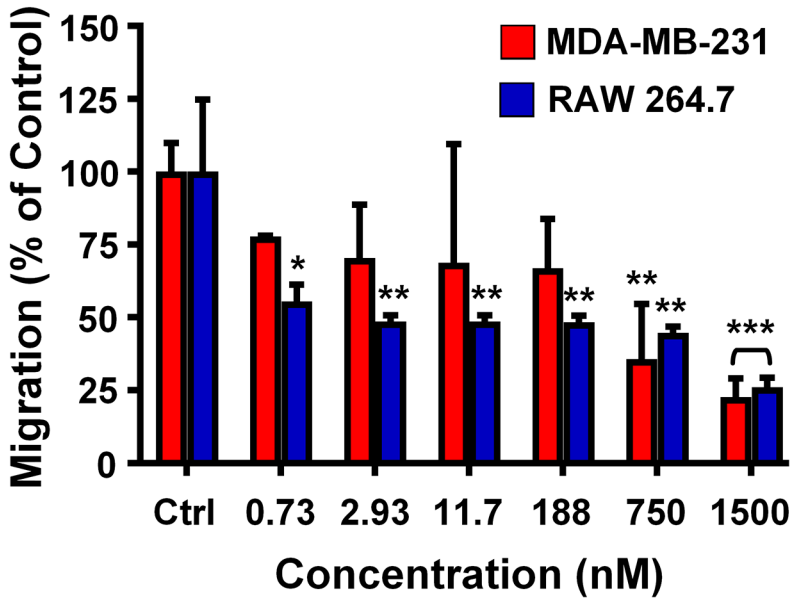

Figure 3. Effect of free, monomeric 58C-scFv on cellular migration.

Transwell migration assay performed with MDA-MB-231 cells and RAW 264.7 cells incubated with increasing concentrations of 58C-scFv. Data are presented as mean ± sd (n=3), *p<0.05, **p<0.01, ***p<0.001 with one-way ANOVA followed by Dunnett's post-test.

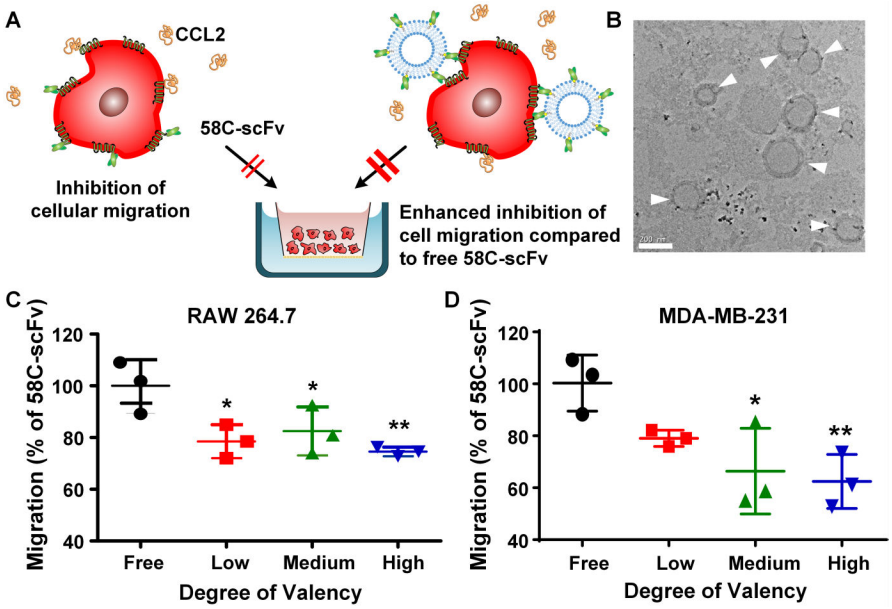

Figure 4. Effect of free, monomeric 58C-scFv and multivalent 58C-scFv on cellular migration.

(**A**) Schematic illustrating the effect of 58C-scFv and liposomal multivalent display of 58C-scFv on cellular migration. **(B)** TEM image of liposomes surface-decorated with 58C-scFv (high degree of valency), scale bar: 200 nm. Transwell migration assay performed with (**C**) RAW 264.7 murine macrophages (**D**) and MDA-MB-231 breast cancer cells. Experiments were performed in triplicate at 88.9 nM. Data are represented as mean ± sd, *p<0.05, **p<0.01, ***p<0.001 with one-way ANOVA followed by Dunnett's post-test.

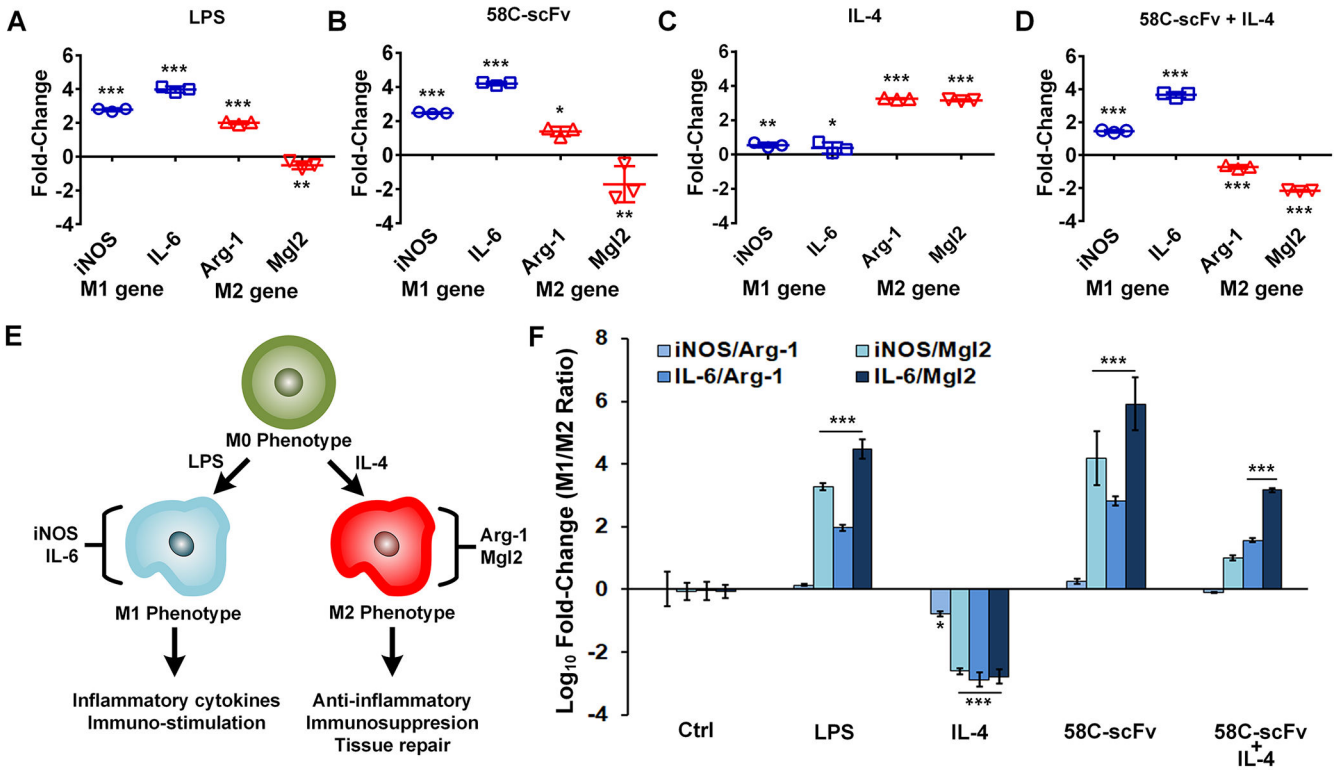

Figure 5. Effect of free, monomeric 58C-scFv on macrophage polarization.

iNOS and IL-6 were used as M1 markers and Arg-1 an Mgl2 were used as M2 markers. Raw 264.7 macrophages treated with (**A**) LPS, (**B**), 58C-scFv, (**C**), IL-4, and (**D**) 58C-scFv + Il4. In **A-C** the genes values were normalized to the untreated control, where **D** was normalized to the IL-4 only control. (**E**) Schematics of macrophage polarization. (**F**) Ratios of M1/M2 marker genes across different conditions normalized to untreated control. Data are represented as mean ± sd, *p<0.05, **p<0.01, ***p<0.001 with one-way ANOVA followed by Dunnett's post-test.

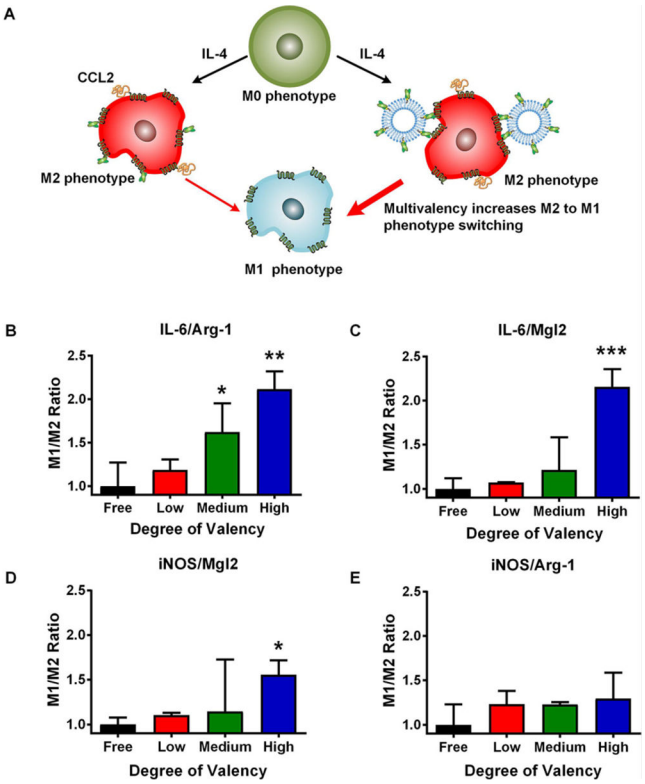

Figure 6. Effect of free, monomeric 58C-scFv and multivalent 58C-scFv on macrophage polarization.

(**A**) Multivalent 58C-scFv induces a stronger M1 phenotype than monomeric, free 58C-scFv. (**B,C,D,E**) The ratios of the M1 markers (IL-6 and iNOS) and M2 markers (Arg-1 and Mgl2) were used to compare the different conditions (M1/M2 ratio). From left to right: 58C-scFv monomers (black); 58C-scFv displayed on liposomes with increasing ligand density: low ligand density (red), medium ligand density (green), and high ligand density (blue). The dose was normalized to the 58C-scFv concentration. The M1/M2 ratio was normalized to the free, monomeric 58C-scFv. Liposome only control was not statistically significant from the untreated control (Supplemental Figure 5). Data are represented as mean ± sd, *p<0.05, **p<0.01, ***p<0.001 with one-way ANOVA followed by Dunnett's post-test.

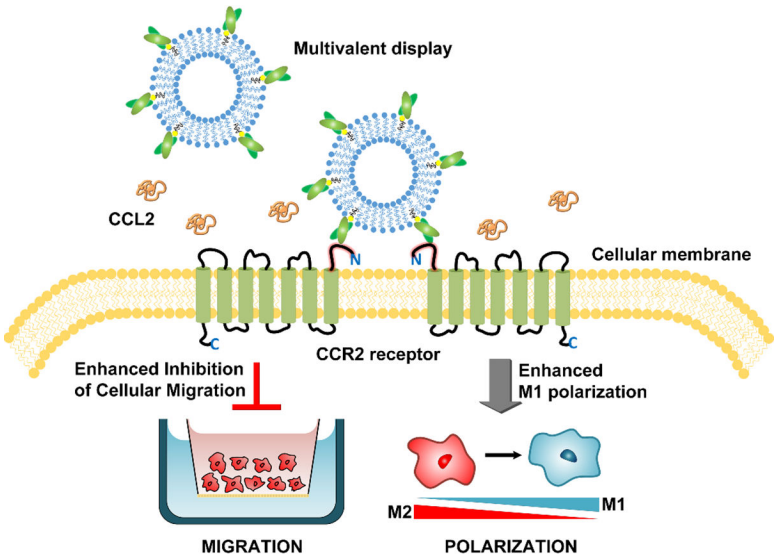

Figure 7. Schematic of multivalent targeting against CCR2 receptors and the observed effects on cellular migration and macrophage polarization.

Multivalent display of 58C-scFv enhanced inhibition of cellular migration and increased M1 polarization of macrophages compared to monomeric, free 58C-scFv.